

# Precise determination of nonlinear function of ion mobility for explosives and drugs at high electric fields for microchip FAIMS

Dapeng Guo,<sup>a</sup> Yonghuan Wang,<sup>a</sup> Lingfeng Li,<sup>a</sup> Xiaozhi Wang<sup>a\*</sup> and Jikui Luo<sup>a,b</sup>

**High-field asymmetric waveform ion mobility spectrometry (FAIMS) separates ions by utilizing the characteristics of nonlinear ion mobility at high and low electric fields. Accurate ion discrimination depends on the precise solution of nonlinear relationships and is essential for accurate identification of ion species for applications. So far, all the nonlinear relationships of ion mobility obtained are based at low electric fields ( $E/N < 65$  Td). Microchip FAIMS ( $\mu$ -FAIMS) with small dimensions has high electric field up to  $E/N = 250$  Td, making the approximation methods and conclusions for nonlinear relationships inappropriate for these systems. In this paper, we deduced nonlinear functions based on the first principle and a general model. Furthermore we considered the hydrodynamics of gas flow through microchannels. We then calculated the specific alpha coefficients for cocaine, morphine, HMX, TNT and RDX, respectively, based on their FAIMS spectra measured by  $\mu$ -FAIMS system at ultra-high fields up to 250 Td. The results show that there is no difference in nonlinear alpha functions obtained by the approximation and new method at low field ( $< 120$  Td), but the error induced by using approximation method increases monotonically with the increase in field, and could be as much as 30% at a field of 250 Td. Copyright © 2014 John Wiley & Sons, Ltd.**

**Keywords:** micro FAIMS; ion mobility nonlinear function; FAIMS spectrum; explosives and drugs

## Introduction

With the increasing terrorist attacks of explosives and transactions of drugs, security agents and law enforcements face tough challenges of detecting hidden explosives and drugs in luggage and mails, on travelers and audiences in stations, airports, stadiums etc.<sup>[1]</sup> In recent years, field asymmetric waveform ion mobility spectrometry (FAIMS) technology has been intensively explored for the applications in detecting and monitoring explosives, chemical warfare<sup>[2]</sup> and illicit drugs<sup>[3]</sup> owing to its high sensitivity, fast detection and simple operation with no need for sample pretreatment. As a mature technology for ion separation in gas phase, FAIMS operated at ambient pressure has been proved to rival a number of mainstream ion detection technologies.<sup>[4]</sup> It utilizes the difference of ion mobility at low and high electric fields to achieve ion separation in gas phase,<sup>[5]</sup> and has advantages in sensitivity and miniaturization compared with conventional ion mass spectrometry (IMS).<sup>[6]</sup> Some theoretical foundations have been established for FAIMS technology. Applications have been explored extensively for the detection of variety of substances such as explosives,<sup>[7]</sup> drugs,<sup>[8]</sup> chemical warfare agents,<sup>[9]</sup> proteomics,<sup>[10,11]</sup> chemical contaminants in drinking water,<sup>[12,13]</sup> biological samples<sup>[14]</sup> and volatile organic compounds etc.<sup>[15]</sup>

However, as a standalone detecting technology, FAIMS is facing several challenges.<sup>[16]</sup> One of them is to seek for methods to link the compensation voltages,  $V_C$ , with ion identities (i.e. FAIMS spectral analysis) accurately. The fundamental issue of this is to precisely solve the nonlinear function of ion mobility.<sup>[17,18]</sup>

The mobility coefficient,  $K$ , is the characteristics of the structure of the ions and the ion-molecule interactions in the channel<sup>[19]</sup> which

is influenced by ion-gas collision and the energy obtained from electric field through ion collisions. The average energy obtained from an electric field is determined by the ratio of the electric field strength,  $E$ , to the gas number density,  $N$ , ( $E/N$ , with the unit of Td,  $1\text{Td} = 10^{-21} \text{Vm}^2$ ). The average energy obtained can be negligible when  $E/N$  is small at low electric fields, and  $K$  can be considered as a constant,  $K_0$ . However, when the electric field increases,  $K$  becomes dependent of  $E/N$ . The relationship can be described in Eqn (1),<sup>[20–22]</sup>

$$K = K_0 \left( 1 + \alpha_2 \left( \frac{E}{N} \right)^2 + \alpha_4 \left( \frac{E}{N} \right)^4 + \dots \right) = K_0^* (1 + \alpha) \quad (1)$$

where  $K_0$  is the mobility coefficient at low field,  $\alpha_2, \alpha_4, \dots$  are specific alpha coefficients of the even powers of the electric field. From symmetry consideration, the mobility coefficient has been expressed as an even power series in  $E/N$ . It is clear that  $\alpha$  is a nonlinear function of the field, and can be expressed in Eqn (2). With the increase in  $n$ , the specific coefficients of the even series decrease rapidly and can be negligible at  $n > 2$ .<sup>[23]</sup> The  $\alpha$  function can be simplified as follows,

\* Correspondence to: Xiaozhi Wang, Department of Information Science & Electronic Engineering, Zhejiang University, Hangzhou 310027, China. E-mail: xw224@zju.edu.cn

<sup>a</sup> Department of Information Science and Electronic Engineering, Zhejiang University, Hangzhou 310027, China

<sup>b</sup> Institute of Renewable Energy and Environment Technology, University of Bolton, Bolton, BL3 5AB, UK

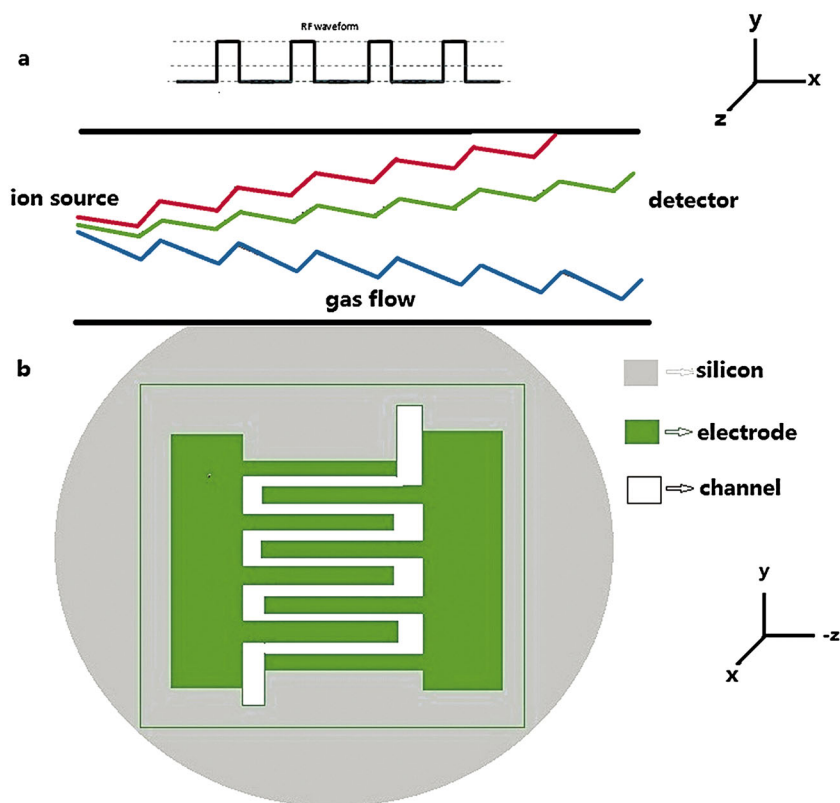


**Figure 1.** Principle of ions separation in channel (a) and a FAIMS chip structure (b).

$$\alpha = \sum_{2n} \alpha_{2n} \left(\frac{E}{N}\right)^{2n} \approx \alpha_2 \left(\frac{E}{N}\right)^2 + \alpha_4 \left(\frac{E}{N}\right)^4 \quad (2)$$

Owing to their importance for the accurate detection of molecules for applications, great efforts have been made to obtain the mobility coefficient, and their specific alpha coefficients  $\alpha_2$  and  $\alpha_4$  or higher for various materials. Using electrospray ionization (ESI) cylindrical FAIMS-MS system, Viehland *et al.*<sup>[24]</sup> obtained the FAIMS spectrum of chloride ions at  $E/N$  up to 65 Td and the corresponding  $\alpha_2$  and  $\alpha_4$  values. The mobility coefficients are in well agreement with the published data obtained

from the drift tube systems at  $E/N$  up to 50 Td. Then his cooperator Guevremont *et al.*<sup>[25]</sup> reported the mobility coefficients of many positive (protonated) and negative (deprotonated) amino acid ions with  $\alpha_2$  and  $\alpha_4$  values at  $E/N$  up to 50 Td in air with the assumption that the transient effects due to the rapid change in field strength are completely negligible. Handy *et al.*<sup>[26]</sup> obtained the alpha functions for  $\text{CH}_3\text{COO}^-$ ,  $\text{CH}_3\text{O}(\text{CO}_2)^-$ ,  $\text{HC}_2\text{O}_4^-$  and  $\text{HSO}_4^-$  using the same method with a similar  $E/N$  value up to 65 Td, and proved that ESI-FAIMS-MS can improve the detection limit of perchlorate significantly compared with that by ESI-MS. Three years later, Buryakov also studied the nonlinear mobility coefficients for the positive ions of aniline, pyridine, benzene *etc.*, and their  $\alpha_2$ ,  $\alpha_4$  and  $\alpha_6$  values.<sup>[27]</sup>

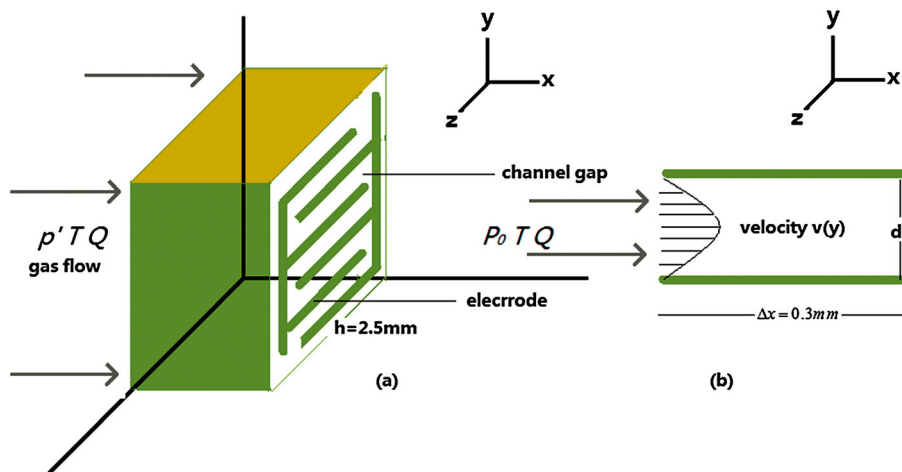


**Figure 2.** Gas flow and chip structure (a) and Poiseuille two dimensional flow model (b).

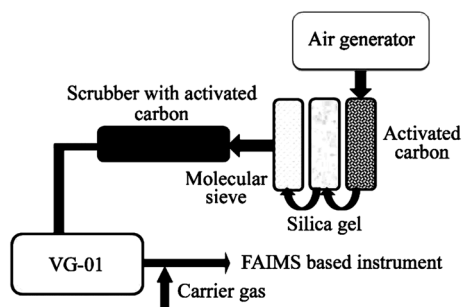


**Figure 3.** Experiment process introduction.

The above researches have all focused on the nonlinear function of mobility coefficients using large cylindrical or planar structure at low fields up to  $E/N=65$  Td. Also for their large systems, the gas number density has been always considered to be constant. Recently a microchip based FAIMS ( $\mu$ -FAIMS) technology has been developed which is much smaller in dimensions and more compact with better sensitivity, and is also suitable for portable applications in field.<sup>[28]</sup> It has been used to detect traces of explosive, additives, organics etc. In this type of  $\mu$ -FAIMS systems, the value of  $E/N$  can easily reach 250 Td<sup>[28]</sup> at ambient pressure. Also the pressure across the microchannels could be very different due to the blockage of gas flow or laminar effect by the microchannels, which may lead to different gas number densities at the entrance and exit. As thus, many assumptions used and conclusions drawn previously from large cylindrical or planar structure FAIMS systems are no longer reliable or valid for this type of  $\mu$ -FAIMS systems. The specific alpha coefficients and nonlinear functions are no longer suitable for practical applications. The  $\mu$ -FAIMS systems have much broader applications for detection of more substances owing to its higher sensitivity and lower cost, but there are no corresponding specific alpha coefficients and nonlinear functions, severely restricting the extended applications of the  $\mu$ -FAIMS systems. Therefore it is necessary to reconsider the situation for the  $\mu$ -FAIMS systems if they are to be explored for widespread applications.

In this paper, we propose a new method to determine  $\alpha_2$  and  $\alpha_4$  coefficients and nonlinear functions of ion mobility. We deduce nonlinear functions based on the first principle and a general model,

and also consider the effect of non-uniform pressure distribution across the microchannels. Based on these, we have successfully obtained the  $\alpha_2$  and  $\alpha_4$  coefficients and nonlinear functions using the experimental results obtained by the  $\mu$ -FAIMS system for cocaine, morphine, HMX, TNT and RDX at high  $E/N$  up to 250 Td. Comparison of the results shows that the alpha coefficients at low field obtained by the new method is very close to those obtained by the approximation method at  $E/N < 120$  Td, but the discrepancy could be as much as 30% at a field up to 250 Td. The analysis method and the deduced equations are all based on a general model, therefore they can be used for other systems, though detailed structure and dimensions of the systems have to be considered carefully in obtaining accurate alpha values and nonlinear functions.

## Theoretical analysis

For ion separation, FAIMS exploits the difference in ion mobility at low and high electric fields. In addition to the application of a DC compensation voltage,  $V_C$ , a bisinusoidal waveform is also used for the dispersion voltage,  $V_D$ , which is synthesized by the summation of a sine wave and its harmonic with an angular frequency,  $\omega$  ( $\omega = f/2\pi$ ,  $f = 25$  MHz for this work). The waveform can be described as a time-dependent function by the following equation,

$$V_D(t) = \frac{V_0}{3} (2 \sin \omega t - \cos 2\omega t) \quad (3)$$

where  $V_0$  is the peak voltage, and  $t$  is the time. The maximum voltage of the dispersion waveform can be obtained by,

$$\frac{dV_D(t)}{dt} = \frac{d}{dt} \frac{V_0}{3} (2 \sin \omega t - \cos 2\omega t) = V_0 \quad (4)$$

when the compensation voltage and dispersion voltage are applied to the electrodes of the FAIMS chip to compensate ion drift under a varying field, which allows some ions to pass through the channel of the systems and to be detected when the drift distance,  $S_d$ , in the  $y$ -direction (as shown in Fig. 1) satisfies Eqn (5) in one duty cycle  $\tau$ .

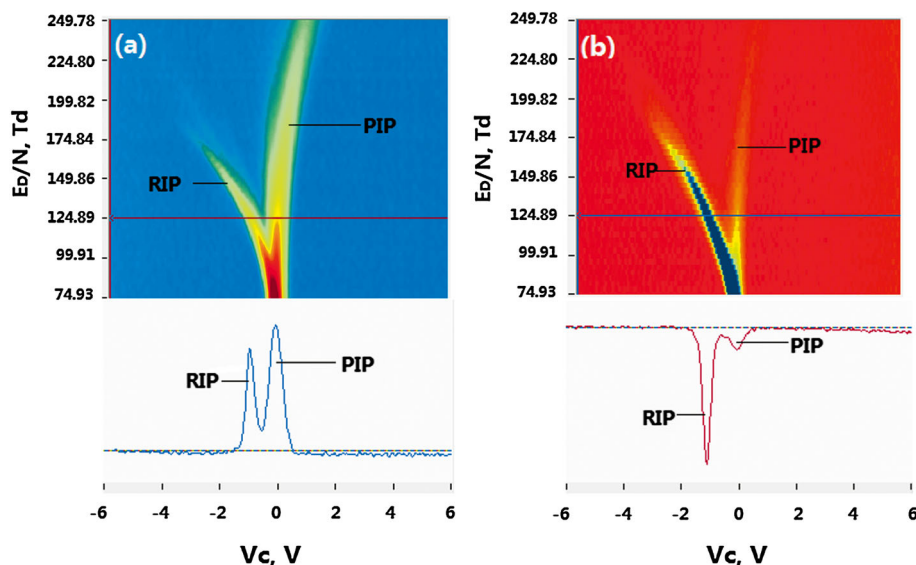


**Figure 4.** FAIMS fingerprint spectrum of cocaine in positive mode (a) and HMX in negative mode (b).

**Table 1.** Experimental parameters

Dispersion voltage (V)	$V_0$	64.2–214
$E_0/N$ (Td)		74.93–249.78
Compensation voltage (V)	$V_C$	–6 – +6
Headspace sampler temperature (°C)	$T$	80
Flow rate of carrier gas (l/min)	$Q$	1.6
Chip channel width (μm)	$d$	35

$$S_d = \frac{K_0}{d} \int_0^\tau (1 + \alpha)(V_C + V_D) dt = 0 \quad (5)$$

where  $K_0 (1 + \alpha)(V_C + V_D)/d$  is the ion drift velocity in the  $y$ -direction. Combined with Eqn (2), we obtain

$$S_d = \frac{K_0}{d} \int_0^\tau \left( 1 + \alpha_2 \left( \frac{V_C + V_D}{Nd} \right)^2 + \alpha_4 \left( \frac{V_C + V_D}{Nd} \right)^4 \right) (V_C + V_D) dt = 0 \quad (6)$$

To solve this equation, it is necessary to know the precise voltages of  $V_D$ ,  $V_C$  for ion species and the gas number density  $N$ .

### Approximation solution

Different asymmetric waveforms have different function forms. Since  $V_C$  plays an insignificant role in low electric field, approximation method has thus been used to solve this equation, especially for complicated waveforms. The following assumptions were normally used in a half-sinusoidal waveform for planar FAIMS.<sup>[18]</sup>

- (i) At low electric field, the specific alpha coefficients  $\alpha_i$  are equal to zero, and the ion mobility coefficient  $K$  is approximately equal to the low field value of  $K_0$ ;
- (ii) The specific alpha coefficients  $\alpha_i$  are only dependent of the dispersion voltage  $V_D$ , and the effect of the compensation voltage  $V_C$  on  $\alpha_i$  is negligible;
- (iii) The gas pressure across the FAIMS channel is constant; hence, the gas number density  $N$  is a constant.<sup>[24,25]</sup>

The approximation method solution for Eqn (6) can be described as follows,

- (i)  $K = K_0$  at low electric field

(ii)

$$\alpha = \alpha_2 \left( \frac{V_C + V_D}{Nd} \right)^2 + \alpha_4 \left( \frac{V_C + V_D}{Nd} \right)^4 \approx \alpha_2 \left( \frac{V_D}{Nd} \right)^2 + \alpha_4 \left( \frac{V_D}{Nd} \right)^4 \quad (7)$$

Combined with Eqn (6), we obtain

$$V_C \tau + \left( \frac{1}{N^2 d^2} \int_0^\tau V_D^3 dt \right) \alpha_2 + \left( \frac{1}{N^4 d^4} \int_0^\tau V_D^5 dt \right) \alpha_4 = 0 \quad (8)$$

This method has been used to calculate the alpha coefficients for ethanol, meta xylene and n-butanol using the experimentally obtained results at low fields for large planar FAIMS systems with half-sinusoidal waveform.<sup>[18]</sup>

Substitute Eqn (3) into Eqn (8), we obtain

$$V_C + \left( \frac{1}{N^2 d^2} \frac{1}{9} V_0^3 \right) \alpha_2 + \left( \frac{1}{N^4 d^4} \frac{55}{486} V_0^5 \right) \alpha_4 = 0 \quad (9)$$

### New method

The conditions for a  $\mu$ -FAIMS system are very different from that of large dimensional cylindrical or planar FAIMS systems. First the channels are much narrower, and the electric field is much higher than those in the conventional cylindrical or planar FAIMS. Second, the low part of the cyclic electric field is not very small compared with the high part of the cyclic electric field in a miniaturized system, and its effect on  $\mu$ -FAIMS systems can no longer be ignored. Furthermore, it is well known that the pressure across a microchannel is not constant due to the blockage of the channel to the flow (hydromechanics) and laminar flow effect. This means the gas number density  $N$  is no longer constant across the microchannels, and the flow is laminar in the parallel microchannels. Therefore, the above listed assumptions become invalid, and the solution is no longer accurate for  $\mu$ -FAIMS. In order to precisely solve the nonlinear functions and to obtain specific alpha coefficients, we need to solve the equation with no assumption and reconsider the factor of the non-constant gas number density,  $N$ , across the microchannels.

**Table 2.** Experimental data used for the extraction of alpha coefficients and nonlinear functions

Sample	Extracted data of $V_C$ to $V_0/(V_C, V_0)$			
Cocaine	(–0.0155, 119.84)	(0.0549, 132.68)	(0.102, 139.10)	(0.196, 147.66)
HMX	(0.0315, 124.12)	(0.0549, 132.68)	(0.172, 154.08)	(0.243, 162.64)
Morphine	(0.219, 158.36)	(0.315, 166.92)	(0.407, 173.34)	(0.56, 181.9)
TNT	(0.00799, 188.32)	(0.0549, 194.74)	(0.102, 201.16)	(0.149, 205.44)
RDX	(–0.0155, 134.82)	(0.0315, 143.38)	(0.243, 164.78)	(0.548, 179.76)

**Table 3.** Calculated  $\alpha_2$  and  $\alpha_4$  coefficients for the five samples

Solution of method	Samples				
$\alpha_2, \alpha_4 (10^{-6} \text{Td}^{-2}, 10^{-10} \text{Td}^{-4})$	Cocaine	HMX	Morphine	TNT	RDX
Approx. method	(0.9720, -0.4583)	(0.2628, -0.1730)	(0.4169, -0.2241)	(0.5493, -0.1132)	(0.8847, -0.3343)
New method	(1.1352, -0.6258)	(0.3026, -0.2342)	(0.4601, -0.2965)	(0.6418, -0.1548)	(1.0291, -0.4550)
Relative error	(14.38%, 26.77%)	(12.99%, 26.13%)	(9.39%, 24.42%)	(14.41%, 26.87%)	(14.03%, 26.53%)
Molecular mass	303.35	291.17	285.35	227.13	222.12

Combining Eqn (3) and Eqn (6), we can obtain

$$V_C + \frac{1}{N^2 d^2} \left( V_C^3 + \frac{15}{18} V_C V_0^2 + \frac{1}{9} V_0^3 \right) * \alpha_2 + \frac{1}{N^4 d^4} \left( V_C^5 + \frac{25}{9} V_C^3 V_0^2 + \frac{10}{9} V_C^2 V_0^3 + \frac{55}{72} V_C V_0^4 + \frac{55}{486} V_0^5 \right) * \alpha_4 = 0 \quad (10)$$

This has been used for simple bisinusoidal waveform by many researchers.<sup>[24,25]</sup> Using experimentally obtained sets of data ( $V_C$ ,  $V_0$  and  $N$ ), we are able to calculate  $\alpha_2$ ,  $\alpha_4$  and the nonlinear function for ion species as discussed below.

Furthermore, it is clear that Eqn (9) is a special case of Eqn (10) at  $V_C = 0$ . It is easy to understand that for a low field,  $V_C$  plays an insignificant role and has almost no impact to the alpha function. Both Eqns (9) and (10) can be represented by,

$$a_i \alpha_2 + b_i \alpha_4 + c_i = 0 \quad (i = 1, 2) \quad (11)$$

where 1, 2 represent the cases of Eqn (9) and (10), respectively,

$$a = \frac{1}{N^2 d^2} \frac{1}{9} V_0^3, \quad b = \frac{1}{N^4 d^4} \frac{55}{486} V_0^5, \quad c = V_C$$

for the approximation method, and

$$a = \frac{1}{N^2 d^2} \left( V_C^3 + \frac{15}{18} V_C V_0^2 + \frac{1}{9} V_0^3 \right), \quad b = \frac{1}{N^4 d^4} \left( V_C^5 + \frac{25}{9} V_C^3 V_0^2 + \frac{10}{9} V_C^2 V_0^3 + \frac{55}{72} V_C V_0^4 + \frac{55}{486} V_0^5 \right), \quad c = V_C$$

for the new method, respectively. Assume

$$Y_i = \frac{b_i}{c_i}, \quad X_i = \frac{a_i}{c_i} \quad (i = 1, 2) \quad (12)$$

and submit it into Eqn (11), we obtain,

$$Y_i = -\frac{\alpha_2}{\alpha_4} X_i - \frac{1}{\alpha_4}, \quad (i = 1, 2) \quad (13)$$

Using experimentally obtained sets of  $V_C$  and  $V_0$  data,  $\alpha_2$  and  $\alpha_4$  can then be calculated, and the nonlinear function for chemicals can be obtained.

### Gas number density N across a microchannel

As mentioned in 2.2, in order to precisely solve the nonlinear function and to obtain specific alpha coefficient for ion species, the carrier gas number density,  $N$ , must be precisely determined. We use the gas number at a standard temperature and pressure (STP) as the reference point which gives,

$$N = \frac{p}{p_0} * \frac{T_0}{T} * N_0 \quad (14)$$

where  $N_0$  is Loschmidt constant ( $N_0 = 2.6868 \times 10^{25}$ ) and  $p_0$  (1 atm) and  $T_0$  (273 K) are the STP pressure and temperature, respectively. The gas number density is  $N = 2.4479 \times 10^{25} \text{ m}^{-3}$  at ambient condition (300 K and 1 atm).

For one measurement,  $T$  in Eqn (14) can be considered to be constant during the experiment owing to its short measurement time; therefore the gas number density becomes solely dependent of pressure. It is known that the velocity of carrier gas flow in a narrow channel is not uniform in both the x- and y-directions as schematically shown in Fig. 2(a) due to the laminar flow effect. The real situation is very complex and does not have a simple analytical form to describe the flow velocity distribution. However the Navier-Stokes equation has been developed to describe the flow velocity which can be solved numerically by computational fluid dynamics. Under some simplified conditions like Poiseuille laminar flow in parallel plates, it can be solved analytically. For a laminar viscous flow between two infinite parallel plates with a constant pressure gradient,  $dp/dx$ , in the x-direction, a gap  $d$  in the y-direction and a dynamic viscosity,  $\mu$ , ( $1.86 \times 10^{-5} \text{ Pa s}$  for air gas at 300 K<sup>[29]</sup>) as shown in Fig. 2 (b), the flow velocity  $v(y)$  is expressed as follows

$$v(y) = \frac{1}{2} \frac{dp}{dx} (y^2 - d^2) \quad (15)$$

Typically the flow velocity distribution has a parabolic profile in the x-y plane. Integrating the velocity,  $v(y)$ , for the y-z plane, we obtain

$$Q = \iint_{S_{y-z}} v(y) ds_{y-z} = -\frac{d^3}{12\mu} * \frac{dp}{dx} * h \quad (16)$$

where  $Q$  is the flow rate,  $h$  is the channel width in the z-direction and  $\mu$  is the dynamic viscosity. This formula implies that the pressures are different at the two sides of a channel. Let  $p'$  be the pressure at the entrance and  $p_0$  that at the exit of the chip channels, respectively. Re-arrange Eqn (16), we obtain the pressure at the entrance as follows

**Table 4.** The nonlinear  $\alpha$  functions of the five substances obtained

Cocaine	$\alpha = 1.1352 \times 10^{-6} (E/N)^2 - 0.6258 \times 10^{-10} (E/N)^4$
HMX	$\alpha = 0.3026 \times 10^{-6} (E/N)^2 - 0.2342 \times 10^{-10} (E/N)^4$
Morphine	$\alpha = 0.4601 \times 10^{-6} (E/N)^2 - 0.2965 \times 10^{-10} (E/N)^4$
TNT	$\alpha = 0.6418 \times 10^{-6} (E/N)^2 - 0.1548 \times 10^{-10} (E/N)^4$
RDX	$\alpha = 1.0291 \times 10^{-6} (E/N)^2 - 0.4550 \times 10^{-10} (E/N)^4$

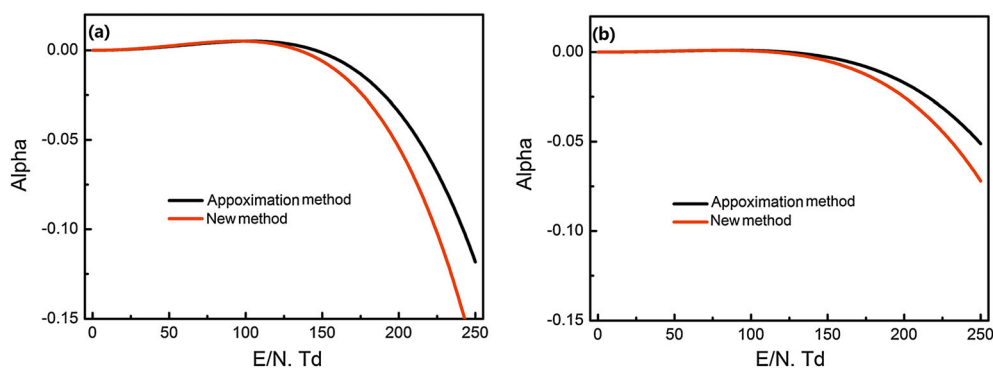


**Figure 5.** Comparison of nonlinear function curves solved by two methods for Cocaine (a) and HMX (b).

$$p' = p_0 + \frac{12\mu Q}{d^3 * h} * \Delta x \quad (17)$$

Here  $\Delta x$  is the chip thickness in the x-direction. The pressure along the channel decreases with the distance. The exit pressure  $p_0$  can be measured by a pressure sensor and controlled by a mass flow controller. It is clear that the pressure difference increases rapidly as the gap,  $d$ , between two plates and the channel width,  $h$ , become smaller, and this should be considered seriously for microchip based FAIMS systems.

The above analyses are based on a general model with no assumption; therefore, the principle and the methodology are applicable for general FAIMS systems. For the application of this new method in other systems, the structure and dimensions of the systems have to be considered accordingly. In the following sections, we will try to obtain  $\alpha_2$ ,  $\alpha_4$  and nonlinear function using the FAIMS spectra measured by the  $\mu$ -FAIMS system for cocaine, morphine, HMX, TNT and RDX.

## Experimental

The  $\mu$ -FAIMS spectrometry system was jointly developed by Zhejiang University and Suzhou Weimu Intelligent System Ltd., China, using the core microchip provided by Owlstone Ltd.<sup>[28]</sup> In our experiments, sample vapor was generated in a headspace sample unit (VG-01), mixed with a flow of clean air (purified by activated carbon and silica gel) gas and was then carried through the FAIMS based instrument with  $^{63}\text{Ni}$  ionization source as shown in Fig. 3.

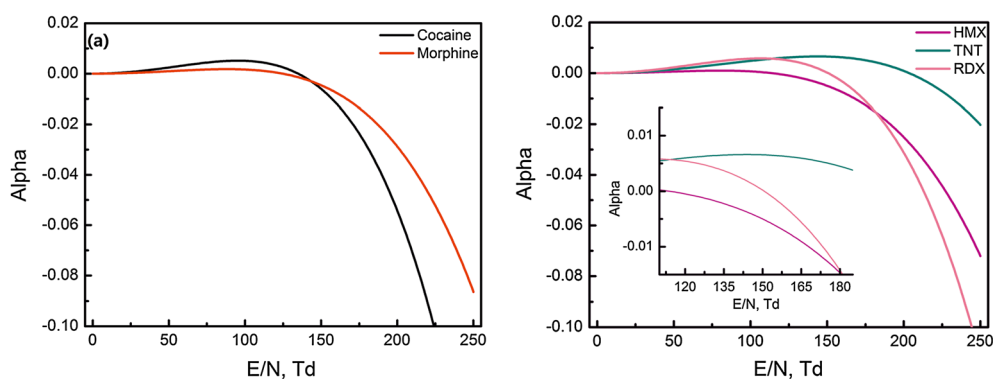


**Figure 6.** Nonlinear function curves of cocaine and morphine (a), and nonlinear function curves of HMX, TNT and RDX (b).

The core part of this instrument is the microchip FAIMS as shown in Fig. 1(b). It consists of serpentine channels with a gap ( $d$  in Eqn (17)) of  $35\ \mu\text{m}$ . The FAIMS chip has an overall dimension of about  $3.25 \times 2.5\ \text{mm}^2$ , a depth ( $\Delta x$  in Eqn (17)) of  $300\ \mu\text{m}$  and the channel width ( $h$  in Eqn (17)) of  $2.25\ \text{mm}$ . The microchip was made of silicon by deep reactive ion etching (DRIE) through the wafer.

For measurements, an RF electric field from  $18,343\ \text{Vcm}^{-1}$  to  $61,143\ \text{Vcm}^{-1}$  ( $V_0 = 30\%$  to  $100\%$  of  $214\ \text{V}$ ) was applied with a duty cycle of  $0.25$ , corresponding to an  $E/N$  range from about  $75\ \text{Td}$  to  $250\ \text{Td}$ . The scanning range of the DC compensation voltage,  $V_C$ , was from  $-6\ \text{V}$  to  $6\ \text{V}$ , as shown in Fig. 4. The detailed optimization of the tests can be found from ref.<sup>[30]</sup> The flow rate of the carrier gas was maintained at  $1.6\ \text{l/min}$  and the temperature in the headspace sampler (VG-01) was controlled at  $80\ ^\circ\text{C}$ . The generated vapor containing sample molecules was introduced by pressurized air, ionized by  $^{63}\text{Ni}$  and carried through the microchannels at room temperature ( $300\ \text{K}$ ). The optimal pressure at the exit of the channel was  $1\ \text{atm}$  ( $\sim 101\ 325 \pm 70\ \text{Pa}$  measured by the pressure sensor (SCX 100 AN)). We have conducted FAIMS measurements for cocaine, morphine, HMX, TNT and RDX under the high  $E/N$  conditions listed in Table 1 using the  $\mu$ -FAIMS instrument. The optimal experimental conditions are listed in Table 1.

## Results and discussions

We used the  $^{63}\text{Ni}$  as the ionization source. The ion reaction mechanism in FAIMS system is the same as that in traditional IMS. According to its ionization mode, in the ionization region, high energy primary electrons are emitted from the ionization source, together with nitrogen, oxygen and water vapor in purified air, and perform

a series of reactions to produce the reactant ions  $H^+(H_2O)_n$  and  $O^{2-}(H_2O)_n$ . The scanning for the positive mode and negative mode is processed at the same time. Drugs like cocaine and morphine containing alkaloid compositions have high proton affinity and can mainly be detected in the positive mode, while explosives such as HMX, TNT and RDX containing nitro compounds have high electron affinities, thus can mainly be detected in the negative mode.<sup>[30,31]</sup> The measured FAIMS spectral results are shown in Fig. 4. Figure 4(a) shows the measured fingerprint spectrum in the positive mode (with cocaine as the example) and Fig. 4(b) shows that in the negative mode (with HMX as the example). The low parts of Fig. 4(a) and 4(b) show the ion current (with a.u. unit) as a function of  $V_C$  for the reactant ion peak (RIP) and product ion peak (PIP)<sup>[28]</sup> at  $E/N = 125$  Td for cocaine and HMX, respectively.

In order to calculate the specific coefficients  $\alpha_2$  and  $\alpha_4$  and obtain the nonlinear functions for the five measured substances, four sets of the resultant data of  $V_C - V_0$  were extracted from the curves of each sample. They are listed in Table 2 for clarification. Before the calculation, we have to reconsider the exact gas number density,  $N$ , and then to compare the difference between the two methods. With the device dimensions and pressure provided above, the pressure,  $p'$ , and the gas number density,  $N'$ , at the entrance of the chip can be calculated using Eqns (17) and (14) as

$$\begin{aligned} P' &= (101325 \pm 69) + 16659 = 117984 \pm 69 \text{ Pa}, \\ N' &= (2.846 \sim 2.849) \times 10^{25} \end{aligned} \quad (18)$$

Here  $p_0 = (101325 \pm 69)$  Pa at the exit of the channels is used which was measured by the pressure sensor (SCX 100 AN). The sensor has a resolution of  $\pm 0.01$  psi (i.e.  $\pm 68.95$  Pa, 1 psi = 6895 Pa), hence can measure the pressure down to the level roughly less than 0.5% of the pressure difference of 16659 Pa across the microchannels. It is clear that the gas number density  $N'$  at the entrance of a microchannel is significantly different from that,  $N = 2.4479 \times 10^{25} \text{ m}^{-3}$ , at the exit of the channel.

For the calculation using the approximation method,  $N$  was used as usually did by others.<sup>[24]</sup> For the new method, a new gas number density will be used as it is significantly different from that of  $N$  due to the pressure variation. Since the pressure decreases linearly along the microchannels as expressed by Eqn (17), we can use the average gas number density,  $N_{new} = (N' + N)/2 = 2.6478 \times 10^{25} \text{ m}^{-3}$  for the new method-based calculation. It is clear that there is an obvious difference in the results obtained by the two different methods. The difference in  $\alpha_2$  could be up to 14%, while that for  $\alpha_4$  could be up to 26%. Substitute the sets of data of  $V_C - V_0$  from Table 2 into Eqn (13), we can obtain the specific alpha coefficients.  $\alpha_2$  and  $\alpha_4$  for the five substances obtained by both the methods are listed in Table 3 for comparison. The units of  $\alpha_2$  and  $\alpha_4$  are  $10^{-6} \text{ Td}^{-2}$  and  $10^{-10} \text{ Td}^{-4}$ , respectively. It has to be pointed out that any uncertainty in dimensions of the microchip could affect the gas numbers significantly as implied by Eqns (17) and (18). However, the dimensions of microchips can now be precisely controlled by modern microfabrication down to nanometers; therefore, the gas number obtained is reliable.

The obtained nonlinear functions for the five substances are summarized in Table 4. Using these functions, we are able to plot the nonlinear function curves at much higher field up to 250 Td, the highest field so far being obtained experimentally for  $\mu$ -FAIMS systems, and to predict their difference and performance. Figure 5 is the comparison of the nonlinear function curves solved by the two methods for cocaine and HMX as the example for the field

up to 250 Td. Both the figures show that the difference in the nonlinear alpha functions obtained by these two methods is small and negligible at  $E/N < 120$  Td, and increases with the  $E/N$  value rapidly. The discrepancy between the two methods increases monotonically, and could be as much as 30% at a field up to 250 Td. This implies that the approximation may have no difference in low field, but is not reliable and would induce substantial errors at high  $E/N$  conditions. The results obtained by the new method would be much more accurate as there is no simplification and assumption used.

In principle, FAIMS does not have very high resolution, and its main advantage is the rapid detection. Although the  $\mu$ -FAIMS system has been used at high electric fields, its advantage of high field nonlinear functions has not been fully utilized. Based on our results, the effective discrimination regions of  $\mu$ -FAIMS systems can be revealed. These nonlinear function curves can help to improve the FAIMS spectral resolutions and to optimize the discrimination conditions by increasing the scanning time in the specific regions selectively, improving the discrimination of ion species without undermining the detection speed. Figure 6 shows the details of the nonlinear function curves at a field of  $E/N < 250$  Td using the specific coefficients  $\alpha_2$  and  $\alpha_4$  obtained for the five substances. Since drugs like cocaine and morphine can be detected easily in the positive mode, while explosives such as HMX, TNT and RDX in the negative mode,<sup>[30,31]</sup> they are plotted in the separated figures. A close look at the curves reveals the difference between the nonlinear function values for the substances measured. Theoretically, the more obvious the difference between the nonlinear function curves, the easier the discrimination for ion separation. As can be seen in Fig. 6(a), cocaine and morphine have a good discrimination region at  $E/N > 170$  Td in the positive mode, and increase with the field, whereas there are two effective regions for the separation of HMX, TNT and RDX in the negative mode in the field region around 144 Td and from  $E/N > 210$  Td, respectively. The latter also increases with the field. These provide a good guidance to set the FAIMS measurement conditions for the detection of chemicals. Based on the above analysis, we can conclude that the optimal separate conditions depend on the nonlinear functions. The more precise the nonlinear function, the more accurate separation conditions are. Thus, accurate solutions for nonlinear functions would improve ion discrimination by FAIMS.

## Summary

Five samples were measured using microchip FAIMS spectrometry system under high  $E/N$  conditions up to 250 Td. A new method has been proposed to solve nonlinear alpha function for ion mobility at high electric fields combined with the consideration of pressure difference across the micro-channels based on the first principle. These have been combined with hydromechanics and experimentally obtained FAIMS spectra for five explosives and drugs to extract the  $V_C - V_0$  spectra at high electric field. The results have been compared with those obtained by the approximation method, and showed that the new method has an obviously advantage over the approximation method with much smaller error at high field. The effects of compensation voltage and channel width  $d$  through gas flow rate and gas number density to the nonlinear function under high  $E/N$  condition have been investigated. Furthermore, we have obtained nonlinear alpha functions for these five species up to field strength of 250 Td. These can help to facilitate FAIMS spectrum database construction and optimize the discrimination

conditions. Moreover, accurate nonlinear function solved by this new method also can be beneficiary in obtaining high precision FAIMS spectrum and accurate discrimination.

### Acknowledgements

The authors acknowledge the financial support from by the National Natural Science Foundation of China (Nos. 61301046 and 61274037), the Applied Research Project of Zhejiang Provincial Sci and Tech Department (2013C31023), the Scientific Research Fund of Zhejiang Provincial Education Department (No. Y201225980), the Fundamental Research Funds for the Central Universities (2012QNA5010) the Research Fund for the Doctoral Program of Higher Education of China (20120101110054 and 20120101110031).

### References

- [1] J. Yinon. Field detection and monitoring of explosives. *TrAC Trends Anal. Chem.* **2002**, *21*, 292.
- [2] G. A. Eiceman, J. A. Stone. Peer Reviewed: Ion Mobility Spectrometers in National Defense. *Anal. Chem.* **2004**, *76*, 390.
- [3] S. Armenta, M. Alcalá, M. Blanco. A review of recent, unconventional applications of ion mobility spectrometry (IMS). *Anal. Chim. Acta* **2011**, *703*, 114.
- [4] E. Nazarov. A journey into DMS/FAIMS technology. *Int. J. Mass Spectrom.* **2012**, *15*, 83.
- [5] B. M. Kolakowski, Z. Mester. Review of applications of high-field asymmetric waveform ion mobility spectrometry (FAIMS) and differential mobility spectrometry (DMS). *Analyst* **2007**, *132*, 842.
- [6] H. Borsdorf, E. G. Nazarov, R. A. Miller. Time-of-flight ion mobility spectrometry and differential mobility spectrometry: A comparative study of their efficiency in the analysis of halogenated compounds. *Talanta* **2007**, *71*, 1804.
- [7] J. G. Bryant, M. Prieto, T. A. Prox, R. A. Yost. Design and evaluation of a novel hemispherical FAIMS cell. *Int. J. Mass Spectrom.* **2010**, *298*, 41.
- [8] P. Hatsis, J. T. Kapron. A review on the application of high-field asymmetric waveform ion mobility spectrometry (FAIMS) in drug discovery. *Rapid Commun. Mass Spectrom.* **2008**, *22*, 735.
- [9] R. Cumeras, I. Gràcia, E. Figueras, L. Fonseca, J. Santander, M. Salleras, C. Calaza, N. Sabaté, C. Cané. Finite-element analysis of a miniaturized ion mobility spectrometer for security applications. *Sens. Actuators B* **2012**, *170*, 13.
- [10] Y. Xia, S. T. Wu, M. Jemal. LC-FAIMS-MS/MS for Quantification of a Peptide in Plasma and Evaluation of FAIMS Global Selectivity from Plasma Components. *Anal. Chem.* **2008**, *80*, 7133.
- [11] J. D. Canterbury, X. Yi, M. R. Hoopmann, M. J. MacCoss. Assessing the Dynamic Range and Peak Capacity of Nanoflow LC – FAIMS – MS on an Ion Trap Mass Spectrometer for Proteomics. *Anal. Chem.* **2008**, *80*, 6888.
- [12] J. Sultan, W. Gabryelski. Structural Identification of Highly Polar Nontarget Contaminants in Drinking Water by ESI-FAIMS-Q-TOF-MS. *Anal. Chem.* **2006**, *78*, 2905.
- [13] B. Ells, D. A. Barnett, R. W. Purves, R. Guevremont. Detection of Nine Chlorinated and Brominated Haloacetic Acids at Part-per-Trillion Levels Using ESI-FAIMS-MS. *Anal. Chem.* **2000**, *72*, 4555.
- [14] J. A. Covington, L. Wedlake, J. Andreyev, N. Ouaret, M. G. Thomas, C. U. Nwokolo, K. D. Bardhan, R. P. Arasaradnam. The detection of patients at risk of gastrointestinal toxicity during pelvic radiotherapy by electronic nose and FAIMS: a pilot study. *Sensors* **2012**, *12*, 13002.
- [15] A. Schumann, C. Lenth, J. Hasener, V. Steckel. Detection of volatile organic compounds from wood-based panels by gas chromatography-field asymmetric ion mobility spectrometry (GC-FAIMS). *Int. J. Mass Spectrom.* **2012**, *15*, 157.
- [16] A. Aksenov, J. Kapron, C. Davis. Predicting Compensation Voltage for Singly-charged Ions in High-Field Asymmetric Waveform Ion Mobility Spectrometry (FAIMS). *J. Am. Soc. Mass Spectrom.* **2012**, *23*, 1794.
- [17] C. Chen, D. Kong, X. Wang, H. Wang, F. Shuang, T. Mei. Peak Profile Analysis in High Field Asymmetric Wave Ion Mobility Spectrometry. *Chin. J. Chem. Phys.* **2011**, *24*, 325.
- [18] C. Zhao, J. Gao, H. You. The Solution of Nonlinear Function of Ion Mobility Based on FAIMS Spectrum Peak Position. *Spectrosc. Spectral Anal.* **2012**, *32*, 2050.
- [19] E. Krylov, E. G. Nazarov, R. A. Miller, B. Tadjikov, G. A. Eiceman. Field dependence of mobilities for gas-phase-protonated monomers and proton-bound dimers of ketones by planar field asymmetric waveform ion mobility spectrometer (PFAIMS). *J. Phys. Chem. A* **2002**, *106*, 5437.
- [20] E. A. Mason, E. W. McDaniel. Transport properties of ions in gases. NASA STI/Recon Technical Report A. Wiley: New York, **1988**, 89.
- [21] E. W. McDaniel, E. A. Mason. Mobility and diffusion of ions in gases. Wiley: New York, **1973**.
- [22] I. A. Buryakov, E. V. Krylov, E. G. Nazarov, U. K. Rasulev. A new method of separation of multi-atomic ions by mobility at atmospheric pressure using a high-frequency amplitude-asymmetric strong electric field. *Int. J. Mass Spectrom. Ion Processes* **1993**, *128*, 143.
- [23] A. A. Shvartsburg, R. D. Smith. Optimum waveforms for differential ion mobility spectrometry (FAIMS). *J. Am. Soc. Mass Spectrom.* **2008**, *19*, 1286.
- [24] L. A. Viehland, R. Guevremont, R. W. Purves, D. A. Barnett. Comparison of high-field ion mobility obtained from drift tubes and a FAIMS apparatus. *Int. J. Mass Spectrom.* **2000**, *197*, 123.
- [25] R. Guevremont, D. A. Barnett, R. W. Purves, L. A. Viehland. Calculation of ion mobilities from electrospray ionization high-field asymmetric waveform ion mobility spectrometry mass spectrometry. *J. Chem. Phys.* **2001**, *114*, 10270.
- [26] R. Handy, D. A. Barnett, R. W. Purves, G. Horlick, R. Guevremont. Determination of nanomolar levels of perchlorate in water by ESI-FAIMS-MS. *J. Anal. At. Spectrom.* **2000**, *15*, 907.
- [27] I. A. Buryakov. Determination of kinetic transport coefficients for ions in air as functions of electric field and temperature. *Tech. Phys.* **2004**, *49*, 967.
- [28] A. A. Shvartsburg, R. D. Smith, A. Wilks, A. Koehl, D. Ruiz-Alonso, B. Boyle. Ultrafast differential ion mobility spectrometry at extreme electric fields in multichannel microchips. *Anal. Chem.* **2009**, *81*, 6489.
- [29] D. R. Lide. *CRC Handbook of chemistry and physics*, 86th ed, 2005–2006, CRC Press: Boca Raton, CRC Press, Boca Raton, **2005**.
- [30] J. Zhang, L. Li, D. Guo, Y. Zhang, Q. Wang, P. Li, X. Wang. Determination of Hazardous Chemicals by Microchip-based Field Asymmetric Ion Mobility Spectrometric Technique. *Chin. J. Anal. Chem.* **2013**, *41*, 986.
- [31] G. A. Eiceman, Z. Karpas. *Ion Mobility Spectrometry*. CRC Taylor and Francis Group: Boca Raton, **2005**.